Indian Journal of Engineering & Materials Sciences
Vol. 32, December 2025, pp. 735-748
DOI: 10.56042/ijems.v32i06.18417

# Characterization of geopolymer concrete with fly ash, micro silica fumes, and waste rubber aggregates

Manoj Kumar Poonia* & Amardeep Boora

Department of Civil Engineering, JUIT, Himachal Pradesh 173 234, India

*Received: 1 April 2025; accepted: 25 October 2025*

Fossil fuel burning and chemical processes involved in the production of cement result in the continuous emission of harmful air pollutants like carbon monoxide, NOx, SOx, etc. Further, these pollutants have hazardous effects on the environment, like depletion of the ozone layer, the greenhouse effect, global warming, etc., exacerbating the situation. Stone is a fundamental component of cement, and its overexploitation has resulted in landscape deterioration, habitat destruction, landscape degradation, water contamination, etc. Geopolymer concrete (GPC) can be used as a substitute for cement concrete in construction applications. The production of GPC utilizing fly ash and micro silica fume has gotten minimal attention. In the present study, GPC has been synthesized at room temperature using Class C fly ash and micro silica fume as substitutes for cement, whereas aggregates have been prepared from waste rubber. The results of mechanical characterization have indicated that the strength parameters enhanced by 3-4% and the microstructural characteristics exhibited effective binding capabilities of GPC, including waste materials. This work serves as a baseline for future research on the incorporation of waste materials into sustainable construction materials.

**Keywords:** Fly ash, Geopolymers, Micro silica fume, Microstructural analysis, Waste rubber aggregate

## 1 Introduction

Use of inexpensive mix design, cement substitution with fly ash or cement-like materials, and alternative binding agents for concrete, such as GPC, are some ways to limit or eliminate cement usage[1]. With its new variety of eco-friendly, affordable building materials, GPC is an excellent alternative to traditional cement concrete. GPC has excellent mechanical properties and significant endurance[2]. Hence, it is necessary to take appropriate action to regulate the consumption of cement in the production of concrete. GPC made from alkali-activated minerals, is one such potential option that may be utilized to completely replace cement in concrete[1-2]. The synthesis of a geopolymer, a general term for a synthetic alkali alumino-silicate material, involves the interaction between a solid alumino-silicate and a concentrated aqueous alkali hydroxide or silicate solution. Geopolymer is named after its founder Joseph Davidovits, a French researcher[3]. Artificial pozzolanic material made from industrial and agricultural by-products such as coal fly ash, steel slag, rice husk ash, nano-silica, and metakaolin supplemented with alumina-silicate has been used to make GPC, which has proven to be a viable substitute to ordinary portland cement (opc) concrete[4-5]. gpc has improved strength, density, temperature effectiveness, tough bonding strength, water tightness, and chemical attack resistance. GPC also decreases the sensitivity to dissolution and the leaching activity of calcium hydroxide[6]. Previous findings express the polymerization process that alumino-silicate composites undergo a chemical reaction with alkaline activity, resulting in a 3D polymeric-chain reaction[7-8]. Although the alkaline activation process is still debated, the chemical composition of the alkali activators and primary sources has a significant impact on the final polymerisation outcomes. When the reaction is accelerated by elevated curing, these polymerization products exhibit notable strength characteristics and may serve as viable alternatives to conventional concrete for the fabrication of pre-cast structures[9]. Industrial by-products (IBP) usage in the field of geopolymer binders significantly reduces energy consumption and greenhouse gas emissions[5, 10]. Further incorporation of materials such as a micro silica fume (MSF) in the production of high-performance concrete enhances the mechanical properties of GPC[11]. The presence of silica in pozzolana interacts with the portlandite formed during the hydration process of OPC which enhances its strength[12]. The use of silica fume-based geopolymers

*Corresponding author (E-mail: 206611@juitsolan.in)

is suitable for situations that need elevated levels of compressive strength. Therefore, the use of silica fume-based geopolymers presents a feasible option for the manufacturing of concrete with superior strength or high-performance concrete, resulting in reduced environmental implications[13]. In a study carried out by the production of GPC was carried out using fly ash as a primary ingredient, with varying proportions of silica fume and the workability, setting time, strength parameters and bonding capabilities were evaluated[14-15].

Most studies focused on geopolymer composites made from a single source material, as curing in dry or steam conditions is a crucial stage in geopolymer synthesis. Class F fly ash activated by alkalis is the sole topic of most research publications. Additionally, from a practical perspective, it is extremely crucial to have the ability to cure GPC to acquire strength at ambient temperature conditions. The flexural behavior and durability of GPC based on ambient cured class C fly ash has been the subject of very little investigation. The flexural behavior of geopolymer reinforced concrete beams based on high calcium fly ash has not been documented in previous research. Nonetheless, this data is critical for structural applications involving reinforced geopolymer concrete. For this reason, the flexural behaviour of high-calcium fly ash geopolymer reinforced concrete beams cured at room temperature was the subject of substantial analytical and experimental research.

In this study, GPC samples are synthesized, both in fresh and hardened states, using class C fly ash (FA) and MSF as a replacement of cement. Further, waste rubber aggregates (WRA) are used as a replacement for coarse aggregates. The prepared samples are characterised for their mechanical and microstructural properties. The samples are investigated for split-tensile strength, compressive strength and flexural strength for mechanical characterization. Scanning electron microscopic analysis (SEM) and X-Ray diffraction (XRD) are carried out for the microstructural and mineralogical characterization. The aim of this research was to examine case studies on GPC usage in a variety of contexts to promote its widespread adoption and raise sustainability consciousness in the building industry. Further, an emphasis on the GPC's mechanical and structural performance is also done to lay the groundwork for future research for the enhancement and applications in various pavement construction practices around the world.

## 2 Materials and Methods

### 2.1 Materials

OPC 43 grade of ACC (brand name) that complies with IS: 12269 (1987) was used for this study. It had no lumps and was dry and powdery. According to IS: 383 (1970), coarse aggregates are defined as graded aggregate with a size of 20 mm. A local merchant and distributor of river sand supplied the fine aggregates utilized in the study. According to IS: 2386 (1986) and IS: 383 (1970), the tests on the course and fine aggregates were carried out and the results were documented in Table 1.

The high calcium (class C) fly ash utilized in the experiments is bought from Angira Bros. Solan. Silica, alumina, iron and calcium make are the main components of FA, which is essentially silicate glass. Some of the minor components are carbon, magnesium, sulphur, sodium and potassium. The XRD patterns of the raw FA were examined at Punjab University, Chandigarh, and are displayed in Fig. 1. There are a few crystalline components that make up the mineral, however the majority of the structure is amorphous. Table 2 represents the chemical compositions of the FA and MSF as determined by XRD analysis. The FA utilized in this experimental study follows the ASTM criteria for chemical composition. Figure 2 shows the SEM

Table 1 — Properties of coarse aggregate.

| S. No | Properties | Coarse Aggregate | Fine Aggregate |
|---|---|---|---|
| 1 | Specific gravity | 2.64 | 2.52 |
| 2 | Fineness Modulus | 3.4 | 5.2 |
| 3 | Bulk density (kg/m$^3$) | 1596.4 | 1882.3 |

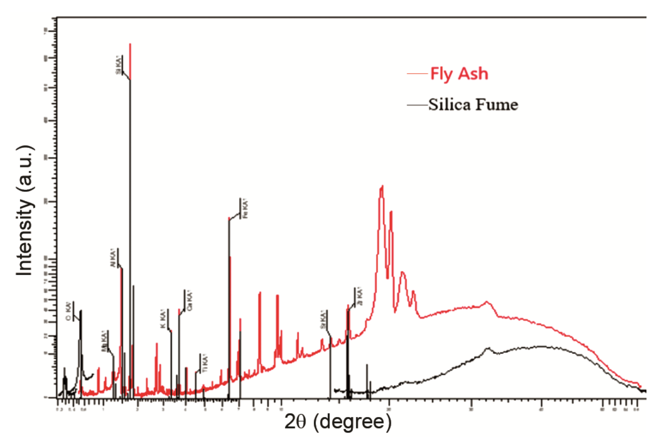


Fig. 1 — XRD analysis of FA and MSF.

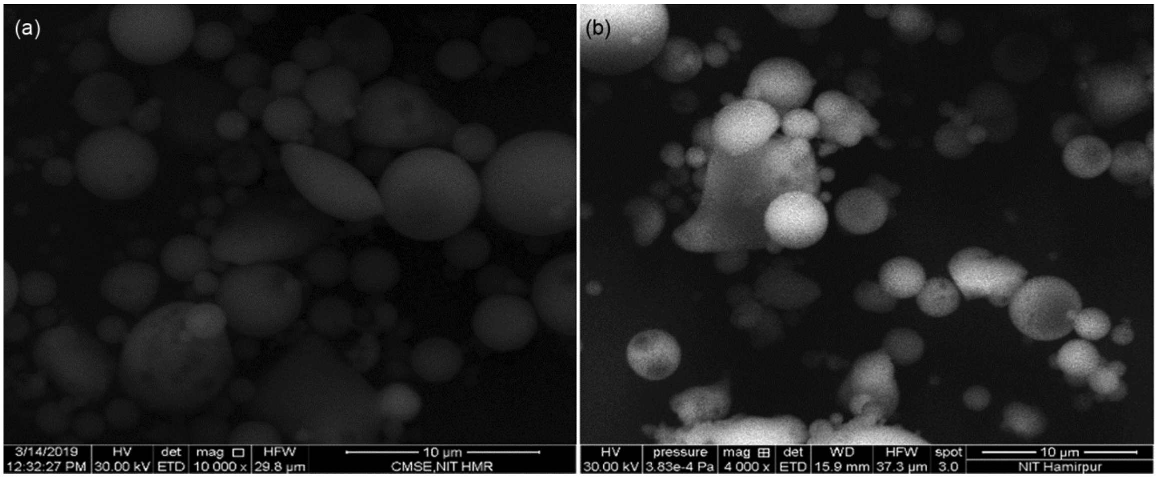


Fig. 2 — SEM analysis of (a) FA and (b) MSF.

Table 2 — Chemical composition of FA and MSF.

| Oxides | Composition, % | |
|---|---|---|
| | Fly Ash | Micro Silica Fume |
| $SiO_2$ | 26.42 | 94.54 |
| $Al_2O_3$ | 16.24 | 0.98 |
| $Fe_2O_3$ | 9.25 | 0.85 |
| CaO | 24.88 | 0.59 |
| $Na_2O$ | 1.56 | 0.46 |
| MgO | 4.28 | 0.62 |
| $SO_3$ | 0.35 | 2.26 |

Table 3 — Properties of FA and MSF.

| S. No | Properties | Fly Ash | MSF |
|---|---|---|---|
| 1. | Specific gravity | 2.62 | 2.46 |
| 2. | Fineness Modulus | 3.4 | 4.3 |
| 3. | Bulk density (kg/m$^3$) | 1596.4 | 1654.3 |

Fig. 3 — WRA used in the experimentation.

analysis of FA and MSF. The image clearly shows that FA particle has a spherical shape. The physical properties of FA and MSF are shown in Table 3.

A major environmental concern has emerged in recent decades due to the non-biodegradable rubber and the resulting disposal dilemma. These issues can be resolved by incorporating this waste material into concrete. So, keeping this in view, Waste Rubber Aggregates (WRA) are used as a substitute of coarse aggregates in the present study. These aggregates were prepared from the MRF brand used tyres, by chopping them into pieces of size 12.5 mm. Every inch of the rubber tyre has been cleaned and dried. Fig. 3 shows the WRA used in the present study. The tests were conducted on the waste rubber aggregates in accordance with IS: 2386 (1986) and IS: 383 (1970), and the results are shown in Table 4.

The alkaline liquid used in the present study is a mixture of sodium silicate and sodium hydroxide solutions having a molarity of 8M and 12M[16-17]. The source material and solution reacted more effectively when sodium silicate solution was added to sodium hydroxide solution as an alkaline activator[18]. To make the sodium hydroxide solution (NaOH), the flakes of sodium hydroxide with a purity level of 98% were dissolved in water. The concentration of the solution, measured in molar (M), was used to adjust the mass of NaOH solids in solution. The present study utilized two alkaline activator solutions including a blend of sodium silicate ($Na_2SiO_3$) and sodium hydroxide (NaOH). The NaOH concentration was at 8 M, while the $Na_2SiO_3$/NaOH mass ratio was set at 2.5. The overall methodology adopted for the present study is depicted in Fig. 4.

**2.2 Nominal design mix**

The mix design for the M40 grade of concrete was carried out in accordance with IRC 44 (2017). The quantity of materials needed for nominal concrete is

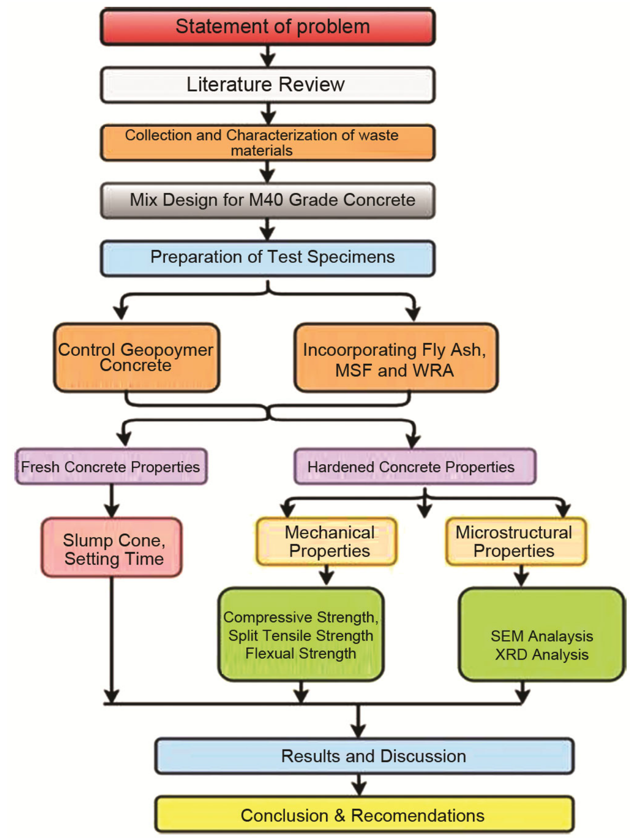


Fig. 4 — Methodology adopted in the study.

Table 4 — Properties of WRA.

| S. No | Properties | Obtained Results |
|---|---|---|
| 1. | Specific gravity | 2.48 |
| 2. | Fineness Modulus | 3.8 |
| 3. | Bulk density (kg/m$^3$) | 1482.7 |

Table 5 — Mix proportions for M40 nominal concrete.

| S. No | Materials | Quantity (kg/m³) |
|---|---|---|
| 1. | Cement | 425 |
| 2. | Water | 195 |
| 3. | Coarse Aggregate | 1122 |
| 4. | Fine Aggregate | 693 |

represented in Table 5. With W/c equal to 0.46 and a mix proportion of 1:1.63:2.64.

The two main processes in preparing a geopolymer mixture are making an alkaline activator solution and combining all the components. About twelve hours prior to the last mixture with the remaining components, the alkaline activator solution was made. The sodium hydroxide and sodium silicate solutions were combined according to the appropriate amount in the lab the day before and allowed to set at room temperature.

It is necessary to allow the mixture to cool before adding it to additional components since it undergoes an exothermic reaction and creates heat. Prior to adding the activator solution, the binder (fly ash), fine and coarse aggregates, and the mixture was dry mixed completely in the mixing pan. Then, a uniform mixture was achieved by gradually adding the premixed alkaline activator solution. The process of mixing and casting specimens of GPC is shown in Fig. 5. Immediate after being prepared, concrete is in its fleeting "fresh" condition. This factor has a significant impact on how the end product acts. Newly formed GPC looked glossy, had a dark hue and becomes solid state.

### 2.3 Replacement with waste materials

This research incorporates additional waste materials into the constant mix proportions. This experimental investigation also makes use of fly ash, WRA and MSF as supplementary waste materials. As a binder, OPC 43 grade was the sole component in the standard combination. For every substitute material concrete is to be mixed with three distinct replacement percentages.

Initial replacement percentages for FA+MSF as 100-0%, 96-4%, 92-8%, 88-12%, and 84-16%. with 8M and 12M alkali activator solutions. By casting and testing specimens ideal for each replacement, the specific surface area improves with a 20% weight increase of silica fume, leading to an increment in the superplasticizer[19]. The workability of concrete is unaffected by the partial cementitious replacement of up to 30% silica fume[20].

At 10%, 20%, 30%, 40%, and 50% by weight, WRA substitutes coarse aggregates. As compared to a control mix, concrete that contains rubber chips as a coarse aggregate has a lower density[21]. The ideal values for the Individual mix proportions were determined by referring to earlier studies that found the percentages for replacing individual components. Replacement levels were used as just a little higher or lower than what would have been ideal.

This study incorporated the three supplementary material replacement combinations to identify the best percentage of replacement of waste materials based on the mechanical and microstructural features after determination of the optimal percentages for each individual replacing material (Industrial by-product). The various mix proportion combinations of GPC are shown in Table 6.

## 3 Results and Discussion

The GPC mixes synthesised with the combinations shown in Table 6 were analysed for the fresh and

Fig. 5 — Casting and mixing of GPC samples.

Table 6 — Mix proportions for GPC.

| S. No | Composition | Acronym |
|---|---|---|
| 1 | Control Mixtures (M40) | N |
| 2 | FA 100% MSF 0% 8M | A1 |
| 3 | FA 96% MSF 4% 8M | A2 |
| 4 | FA 92% MSF 8% 8M | A3 |
| 5 | FA 88% MSF 12% 8M | A4 |
| 6 | FA 84% MSF 16% 8M | A5 |
| 7 | FA 100% MSF 0% 12M | B1 |
| 8 | FA 96% MSF 4% 12M | B2 |
| 9 | FA 92% MSF 8% 12M | B3 |
| 10 | FA88% MSF 12% 12M | B4 |
| 11 | FA 84% MSF 16% 12M | B5 |
| 12 | FA 92% MSF 8% WRA 10% 8M | C1 |
| 13 | FA 92% MSF 8% WRA 20% 8M | C2 |
| 14 | FA 92% MSF 8% WRA 30% 8M | C3 |
| 15 | FA 92% MSF 8% WRA 40% 8M | C4 |
| 16 | FA 92% MSF 8% WRA 50% 8M | C5 |
| 17 | FA 88% MSF 12% WRA 10% 12M | D1 |
| 18 | FA 88% MSF 12% WRA 20% 12M | D2 |
| 19 | FA 88% MSF 12% WRA 30% 12M | D3 |
| 20 | FA 88% MSF 12% WRA 40% 12M | D4 |
| 21 | FA 88% MSF 12% WRA 50% 12M | D5 |

mechanical properties. The properties considered under fresh criteria are setting time, workability, sorptivity and water absorption. For mechanical (hardened) properties, compressive strength, split tensile strength and flexural strength were considered.

### 3.1 Fresh properties of mixes

Workability is one of the key qualities of freshly mixed concrete that influences the strength of the final product. The workability of concrete is determined by how easily it can be placed while yet exhibiting resistance to segregation[22]. Slump values for high calcium GPC of varied molarities were found to be comparable with regular concrete in this case. The slump cone test was used to measure the consistency of the GPC and determine its workability. The Indian standard criteria IS:1199 (1959) was used to determine the slump range. Manual strokes were applied in three equal thicknesses to compact the new concrete in the cylindrical steel moulds. The addition of water makes the GPC more workable if it is found to be hard[23].

According to ASTM C403, the setting time of geopolymer paste was found to be the same as that of regular concrete. Setting time is an indication of the development of cementitious characteristics and attainment of a specific degree of penetration resistance[24]. Based on the level of needle penetration in the geopolymer paste, setting times were assessed using Vicat's equipment. The first setting time is the amount of time that passes from the addition of water to the cement until the paste begins to lose its flexibility[25]. From the time water introduced to the cement until the paste entirely loses its plasticity, this is the time which is considered as final setting time.

The rate of water absorption through unsaturated concrete under capillary suction is measured by sorptivity. The lower the water sorptivity index, the better is the potential durability of the concrete[26-27]. Cylindrical specimens of 100 mm in diameter and 50 mm in height (ASTM C-642 standard) were subjected to the sorptivity tests. After 45 days of casting, the cylinders were submerged in water to cure. The samples being dried in an oven at 110°C for 24 hours after curing. The specimens were submerged in water up to 5 mm above their bases, and to ensure that the water flow in one direction only, the specimens' periphery was adequately sealed with a non-absorbent covering. The amount of water that was absorbed throughout a 30-minute period was recorded. Equation (1), which are provided below, were used to compute the sorptivity coefficient.

$$S = \frac{I}{\sqrt{t}} \quad \ldots(1)$$

where, S = Sorptivity (mm); I = cumulative absorption; t = Elapsed time (minutes).

The specimens were weighed before and after submerging in water once their mass had stabilized. The cylinder's dry weight ($W_1$) was recorded. A subsequent 3.5 hours were spent immersing the specimen in water at 85°C. The cylinder's wet weight ($W_2$) was then recorded. The absorption of water was determined using Equation (2).

$$\%\, Water\ Absorption = \frac{W_1 - W_2}{W_1} x 100 \quad \ldots(2)$$

where, $W_1$ = Oven dry weight of cylinder (gm); $W_2$ = Wet weight of cylinder (gm) after 3.5 hours.

The fresh properties of the geopolymer mixes are summarised in Table 7. It can be seen that the workability and setting of GPC is generally less than the nominal concrete. This is due to more water retention capabilities of FA mixed with MSF. Further, this led to and increased water absorption and sorptivity values as compared to M40 grade of concrete mix. The individual variations will further be analysed with the mechanical properties of GPC mixes.

Table 7 — Fresh properties for GPC.

| Geopolymer Mix | Slump (mm) | Final Setting Time (Min) | Sorptivity (mm/min$^{0.5}$) | Water Absorption % |
|---|---|---|---|---|
| N | 115 | 306 | 0.215 | 0.68 |
| A1 | 118 | 220 | 0.162 | 1.12 |
| A2 | 112 | 215 | 0.168 | 1.18 |
| A3 | 109 | 208 | 0.175 | 1.22 |
| A4 | 105 | 205 | 0.178 | 1.26 |
| A5 | 98 | 202 | 0.182 | 1.31 |
| B1 | 117 | 216 | 0.171 | 1.15 |
| B2 | 113 | 211 | 0.175 | 1.22 |
| B3 | 108 | 205 | 0.179 | 1.29 |
| B4 | 102 | 198 | 0.183 | 1.33 |
| B5 | 95 | 192 | 0.189 | 1.38 |
| C1 | 115 | 198 | 0.179 | 1.28 |
| C2 | 118 | 192 | 0.182 | 1.32 |
| C3 | 121 | 184 | 0.188 | 1.37 |
| C4 | 119 | 182 | 0.195 | 1.41 |
| C5 | 112 | 177 | 0.198 | 1.49 |
| D1 | 119 | 195 | 0.181 | 1.36 |
| D2 | 121 | 188 | 0.185 | 1.42 |
| D3 | 126 | 175 | 0.189 | 1.49 |
| D4 | 124 | 172 | 0.193 | 1.53 |
| D5 | 120 | 166 | 0.195 | 1.61 |

### 3.2 Mechanical properties

Class C fly ash-based GPC specimens measuring size 150×150×150 mm were subjected to compressive strength testing. A combination of fine aggregate, coarse aggregate, an alkaline solution, and high calcium class C fly ash was used in the synthesis. The three-layer GPC cubes were produced in compliance with IS: 10080 (1982). A tamping rod was used to compress each layer thoroughly. The top surface was protected from evaporation by covering it with a polythene sheet after compression. Demoulding the concrete cubes was done after four hours of casting[28]. After that, it was allowed to cure at room temperature. By following these processes, GPC cubes underwent hydraulic compression testing in accordance with IS: 4031-1982 (Part 6). Equation (3) is used to compute the compressive strength at failure.

$$Compressive\ Strength = \frac{Ultimate\ Compressive\ Load}{Area\ of\ Cross\ Section\ of\ Specimen} \quad \ldots(3)$$

One indirect way to find the concrete's tensile strength is by using split tensile strength. In compliance with IS: 5816 (1999), the split tensile strength test was conducted. At room temperature, 150×300 mm cylindrical specimens were casted and allowed to cure. To make sure the cylinders were in the same axial plane, central lines were painted on both faces. The Compression Testing Machine was used to position the specimens. The purpose of this test is to determine whether a concrete specimen can withstand tensile strains caused by a compressive force or not. A diametrical compressive load was applied gradually, along the cylinder's height to determine the ultimate load at failure or rupture. Equation (4) was used to compute the split tensile strength.

$$f_{st} = \frac{2P}{\pi LD} \quad \ldots(4)$$

where, $f_{st}$ = Split tensile strength (N/mm$^2$); D = Cylindrical specimen's diameter (mm); P = Maximum load before failure (N); L= length of the cylinder (mm).

The tensile strength of unreinforced concrete is determined by the concrete's flexural strength. The flexural strength of concrete is usually around 10% to 20% of its compressive strength. The Rupture Modulus is a unit for measuring concrete's flexural strength. The flexural strength of concrete is often determined by tests like the three-point load test (ASTM C78) or the centre point load test (ASTM C293). It is used to test the strength of concrete slabs and pavements and is an ingredient in concrete design mixes. Equation (5) was used to compute the flexural strength as specified in IS: 516 (Part 1/ Sec 1) - 2021.

$$f_{bt} = \frac{Pl}{bd^2} \quad \ldots(5)$$

where, $f_{bt}$ = Flexural strength (N/mm$^2$); d = Cylindrical specimen's diameter (mm); P = Maximum load before failure (N); b= Width of the sample (mm).

A total six concrete cubes were prepared for every concrete combination. From each combination, a total of three specimens were selected for compressive strength, split tensile strength and flexural strength testing on the seventh day, while the remaining three specimens were tested after 28 days. The average of the three readings within each set of specimens was calculated for analysis. As to IS: 516-1959 (2004), concrete has rapid strength development in the first stages after being poured, with about 90% of its maximum strength attained within only 14 days for M40 mix. After the concrete has achieved a strength of 99% within a 28 days period, it continues to progressively enhance its strength. The strength parameters of FA used as a substitute for the cementitious materials is shown in Table 8. The test results show that when FA+MSF with 8M alkaline activator solution are used as a substitute for cementitious material in varying ratios, increasing the amount of MSF in the mix leads to a decrease in the compressive strength of the concrete. Utilizing MSF as a substitute for 8% (A3) of the material leads to a decrease in compressive strength of 2.5%. Similarly, the use of MSF as a substitute material at a proportion of 12% (A4) results in a decrease of compressive strength by 7% in 28 days. Utilizing MSF as a waste material, substituting 16% (A5) of the initial material, leads to a 17.2% decrease in compressive strength as depicted in Fig. 6.

The split tensile and flexural strength of FA used as a substitute for the cementitious materials is shown in Table 8. It has been shown via research that there is an inverse relationship between the percentage of FA+MSF (8M) and the split tensile strength of the specimen, i.e. the strength decreases as the amount of MSF in the specimen increases. It was noticed that there was a 5.5% drop in 28 days split tensile strength when 8% of the MSF was replaced with 92% FA (A3) content as shown in Fig. 6.

The empirical data shown in Table 8 illustrate that the use of FA as a replacement for cement results in a decrease in the 28 days flexural strength of concrete. When FA+MSF is used as a substitute material at a rate of 92-8%, the flexural strength decreases by 2%. However, if the replacement rate is increased to 88-12%, the flexural strength falls even more,

Table 8 — Strength parameters of mixes with FA+MSF (8M) substitution.

| S. No | Mix | Compressive Strength (N/mm$^2$) | | Split Tensile Strength (N/mm$^2$) | | Flexural Strength (N/mm$^2$) | |
|---|---|---|---|---|---|---|---|
| | | 7$^{th}$ Day | 28$^{th}$ Day | 7$^{th}$ Day | 28$^{th}$ Day | 7$^{th}$ Day | 28$^{th}$ Day |
| 1. | N | 29.2 | 43.4 | 2.52 | 3.67 | 3.85 | 4.94 |
| 2. | A1 | 28.4 | 41.6 | 2.48 | 3.58 | 3.74 | 4.88 |
| 3. | A2 | 27.3 | 39.8 | 2.41 | 3.48 | 3.65 | 4.74 |
| 4. | A3 | 24.3 | 38.1 | 2.34 | 3.39 | 3.54 | 4.66 |
| 5. | A4 | 23.5 | 36.8 | 2.28 | 3.28 | 3.42 | 4.51 |
| 6. | A5 | 22.7 | 35.9 | 2.18 | 3.15 | 3.29 | 4.38 |

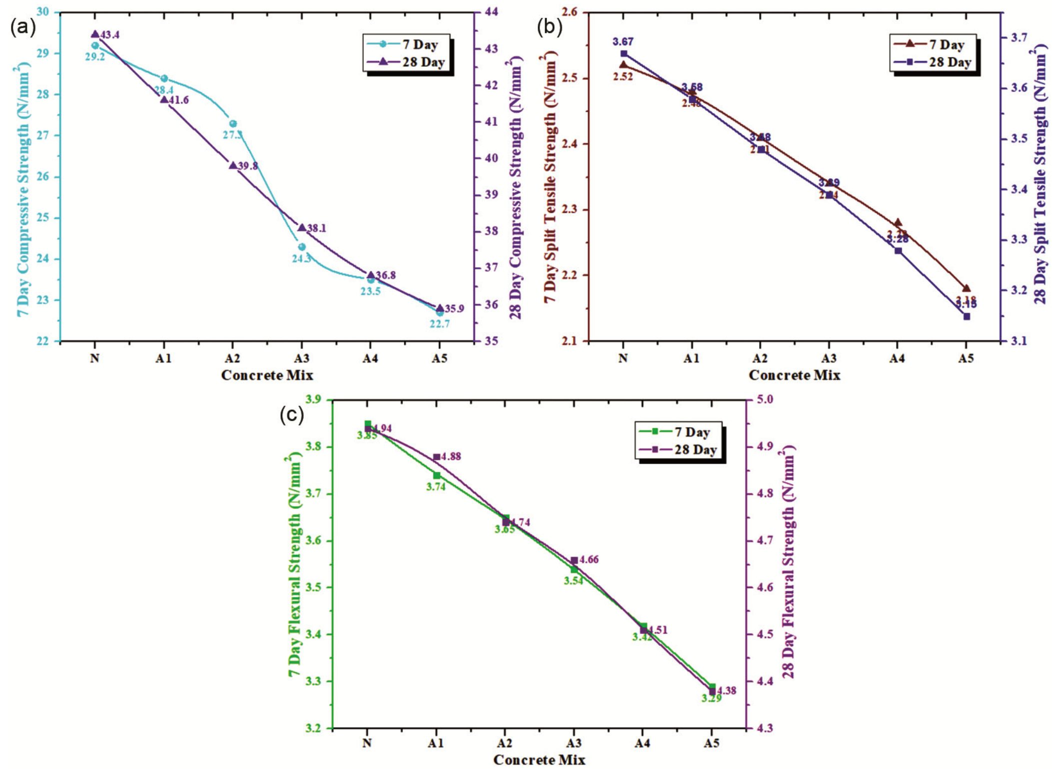


Fig. 6 — Effect on strength parameters of FA+MSF (8M) replacement on (a) Compressive strength, (b) Split tensile strength and (c) Flexural strength.

specifically by 6%. The effect on strength parameters of FA+MSF (8M) replacement is shown in Fig. 6.

### 3.3 Strength parameters of FA+MSF (12M)

Based on the results, the addition of cement replacement with a replacement level of 92-8% leads to a 5% increase in cube strength as shown in Fig. 7. Similarly, a replacement level of 88-12% resulted 8% increase in 28 days cube compressive strength, as shown in Table 9 and represented in Fig. 7. However, it is crucial to recognize that as the proportion of MSF replacement increases, there is a corresponding reduction in the pliability of the concrete.

Table 9 illustrates that the 28 days split tensile strength, shown in Fig. 7, increases by 7% when the FA+MSF (12M) concentration is increased from 96-4% (B2) to 92-8% (B3), as shown in Fig. 7. Further increments in MSF concentration led to an elevation in the split tensile strength measurement. When 60-40% (B5) of FA+MSF (12M) was used instead of cement, the split tensile value showed an estimated 12% enhancement. Nevertheless, the variation is minimal, and the workability of the mixture steadily declined.

The flexural strength decreases by 4% with the addition of 20% WRA in A3 design mix, as shown in Fig. 7, when coarse aggregates are replaced with these materials, as given in Table 9. Also, whenever the ratio of WRA goes above 30% to 50%, the 28 days flexural strength keeps going down, from 7% to 10%.

#### *3.3.1 Strength parameters of FA+MSF+WRA (8M)*

The substitution of WRA in place of coarse aggregates was done in percentages of 20%, 30%, 40%, 50% and 100 % by weight. Strength parameters at 7 days and 28 days were measured by casting cubes and curing them adequately. The results represented in Table 10 shows a reduction in strength of 3.5% was seen when 20% of WRA was substituted in C3 design mix, while a 5% decrease in strength was observed with a substitution of 30% WRA. When the WRA were substituted with 40%, the strength was further reduced to 6.4% similar to the earlier studies[29-30].

Figure 8 demonstrates that when coarse aggregate is replaced with 20% WRA in the A3 design mix, there is a little reduction in 28 days split tensile strength. However, when coarse aggregate is replaced with 50% WRA, the strength drops by 8%. When 20% WRA are used in place of the coarse aggregates, the maximum strength is achieved. When utilized as a replacement for coarse aggregates WRA displays unique behaviour.

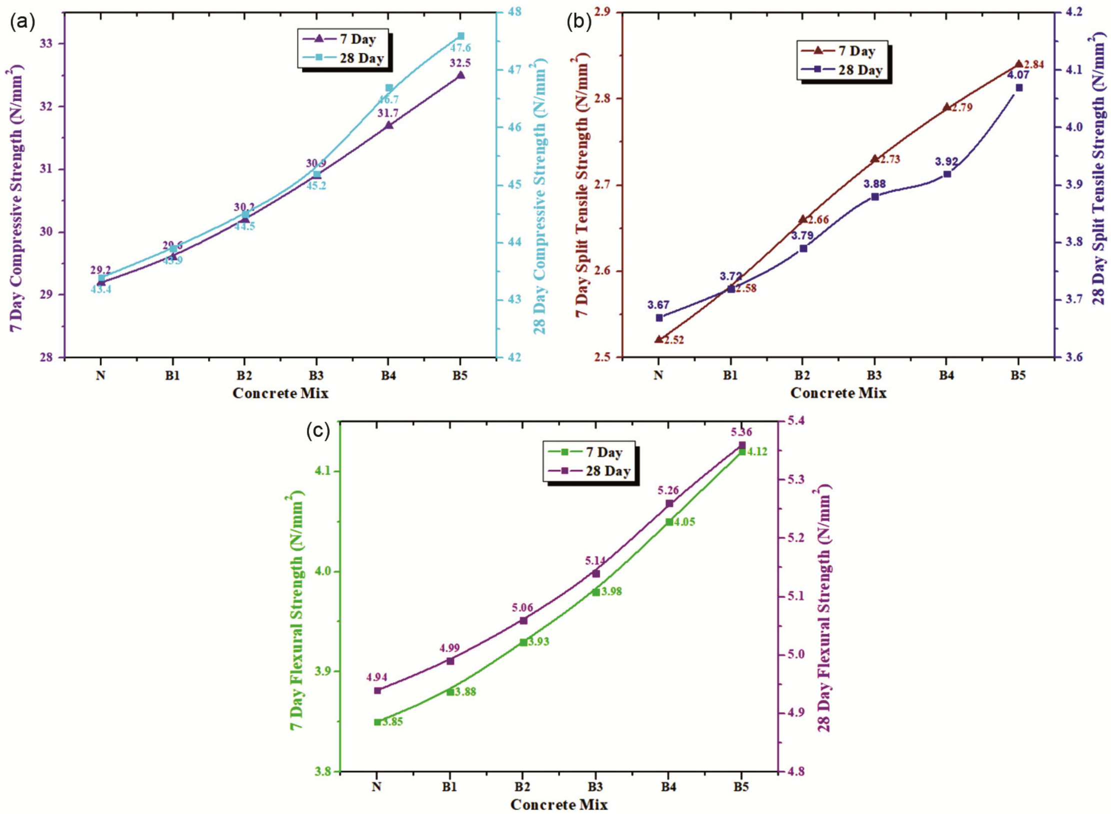


Fig. 7 — Effect on strength parameters of FA+MSF (12M) replacement (a) Compressive strength, (b) Split tensile strength and (c) Flexural strength.

Table 9 — Strength parameters of mixes with FA+MSF (12M) substitution.

| S. No | Mix | Compressive Strength ($N/mm^2$) | | Split Tensile Strength ($N/mm^2$) | | Flexural Strength ($N/mm^2$) | |
|---|---|---|---|---|---|---|---|
| | | $7^{th}$ Day | $28^{th}$ Day | $7^{th}$ Day | $28^{th}$ Day | $7^{th}$ Day | $28^{th}$ Day |
| 1 | N | 29.2 | 43.4 | 2.52 | 3.67 | 3.85 | 4.94 |
| 2 | B1 | 29.6 | 43.9 | 2.58 | 3.72 | 3.88 | 4.99 |
| 3 | B2 | 30.2 | 44.5 | 2.66 | 3.79 | 3.93 | 5.06 |
| 4 | B3 | 30.9 | 45.2 | 2.73 | 3.88 | 3.98 | 5.14 |
| 5 | B4 | 31.7 | 46.7 | 2.79 | 3.92 | 4.05 | 5.26 |
| 6 | B5 | 32.5 | 47.6 | 2.84 | 4.07 | 4.12 | 5.36 |

The flexural strength decreases by 4% with the addition of 20% WRA in A3 design mix, as shown in Fig. 8. Also, whenever the ratio of WRA goes above 30% to 50%, the 28 days flexural strength further reduces from 7% to 10%.

### *3.3.2 Strength parameters of FA+MSF+WRA (12M)*

The percentages of coarse aggregates were replaced with WRA ranged from 10% to 50%. On days 7 and 28, the casted cubic specimens were tested for strength. Table 11 shows that substitution of 30% WRA resulted in 4% increase in strength of B4 design mix. Figure 9 shows that increasing the replacement ratio to 30% of WRA resulted in 12% improvement in 28 days compressive strength. The strength showed an additional 15% improvement when 40% WRA was used. Figure 9 shows that using more than 50% WRA instead of coarse aggregate significantly reduced the mixes' workability.

Figure 9 shows that tensile strength varied by 8-10% when WRA was added at 30-40% concentration. No change in workability was noted, even though the highest strength gain occurred at 50% replacement. Figure 9 shows that when WRA is used as coarse aggregates, the split tensile strength increases, suggesting that WRA may be successfully used as a coarse aggregate substitute.

Figure 9 shows 2% increase in 28 days flexural strength is achieved when 20% WRA is used in place of the coarse aggregate. The flexural strength also

Table 10 — Strength parameters of mixes with FA+MSF+WRA (8M) substitution.

| S. No | Mix | Compressive Strength (N/mm$^2$) | | Split Tensile Strength (N/mm$^2$) | | Flexural Strength (N/mm$^2$) | |
|---|---|---|---|---|---|---|---|
| | | 7$^{th}$ Day | 28$^{th}$ Day | 7$^{th}$ Day | 28$^{th}$ Day | 7$^{th}$ Day | 28$^{th}$ Day |
| 1. | N | 29.2 | 43.4 | 2.48 | 3.58 | 3.85 | 4.94 |
| 2. | C1 | 28.6 | 42.8 | 2.42 | 3.51 | 3.78 | 4.86 |
| 3. | C2 | 27.5 | 41.9 | 2.35 | 3.43 | 3.67 | 4.74 |
| 4. | C3 | 26.6 | 41.2 | 2.27 | 3.33 | 3.54 | 4.65 |
| 5. | C4 | 25.2 | 40.6 | 2.21 | 3.24 | 3.41 | 4.49 |
| 6. | C5 | 24.5 | 39.4 | 2.13 | 3.18 | 3.32 | 4.37 |

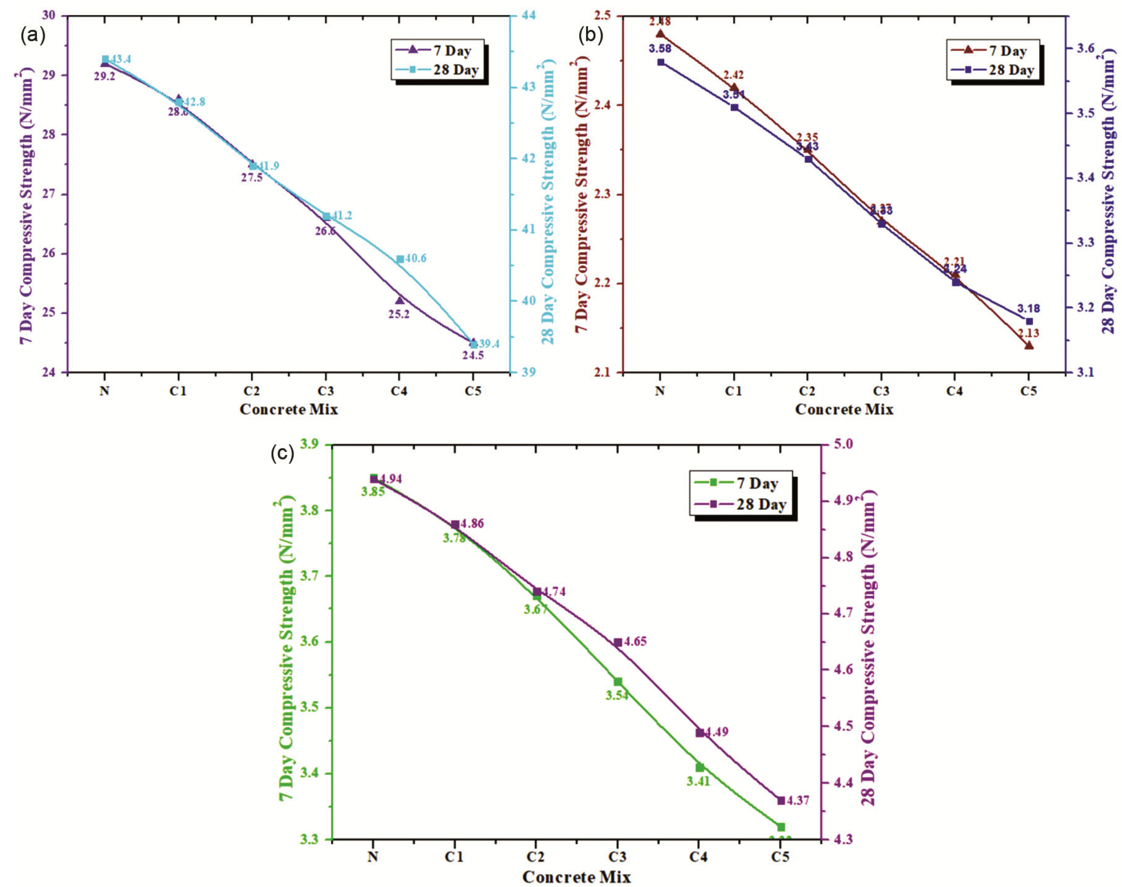


Fig. 8 — Effect on strength parameters of FA+MSF+WRA (8M) replacement (a) Compressive strength, (b) Split tensile strength and (c) Flexural strength.

increases noticeably by around 6% when the replacement is raised to 30% of WRA. A notable and unexpected improvement of 9% in flexural strength is observed when 50% WRA is used as material substitution, as illustrated in Fig. 9. Nevertheless, the mixture's workability diminished noticeably.

***3.3.3 Mechanical properties of mixes***

The supplementary materials have a compressive, split-tensile and flexural strength that is adequate, which is higher than the strength of the nominal mix. At a ratio of 92-8%, it has been demonstrated that this substitution of FA+MSF replacement for cement and the replacement of coarse aggregate with WRA is more acceptable. However, increasing the percentage of WRA results in a further reduction in the material's workability. The replacement of cementitious material with MSF improves the quality of the mixture[2, 31-32]. The utilization of a large percentage of MSF is associated with a number of downsides, including its high cost and the decreased workability. Based on the results of the characterization, it was analysed that strength of the concrete mix, which consists of FA and MSF in addition to other components, was

Table 11 — Strength parameters of mixes with FA+MSF+WRA (12M) substitution.

| S. No | Mix | Compressive Strength (N/mm$^2$) | | Split Tensile Strength (N/mm$^2$) | | Flexural Strength (N/mm$^2$) | |
|---|---|---|---|---|---|---|---|
| | | 7$^{th}$ Day | 28$^{th}$ Day | 7$^{th}$ Day | 28$^{th}$ Day | 7$^{th}$ Day | 28$^{th}$ Day |
| 1. | N | 29.2 | 43.4 | 2.48 | 3.58 | 3.85 | 4.94 |
| 2. | D1 | 29.8 | 44.1 | 2.42 | 3.51 | 3.78 | 4.86 |
| 3. | D2 | 30.6 | 44.9 | 2.35 | 3.43 | 3.67 | 4.74 |
| 4. | D3 | 31.3 | 45.6 | 2.27 | 3.33 | 3.54 | 4.65 |
| 5. | D4 | 32.4 | 46.5 | 2.21 | 3.24 | 3.41 | 4.49 |
| 6. | D5 | 33.3 | 47.3 | 2.13 | 3.18 | 3.32 | 4.37 |

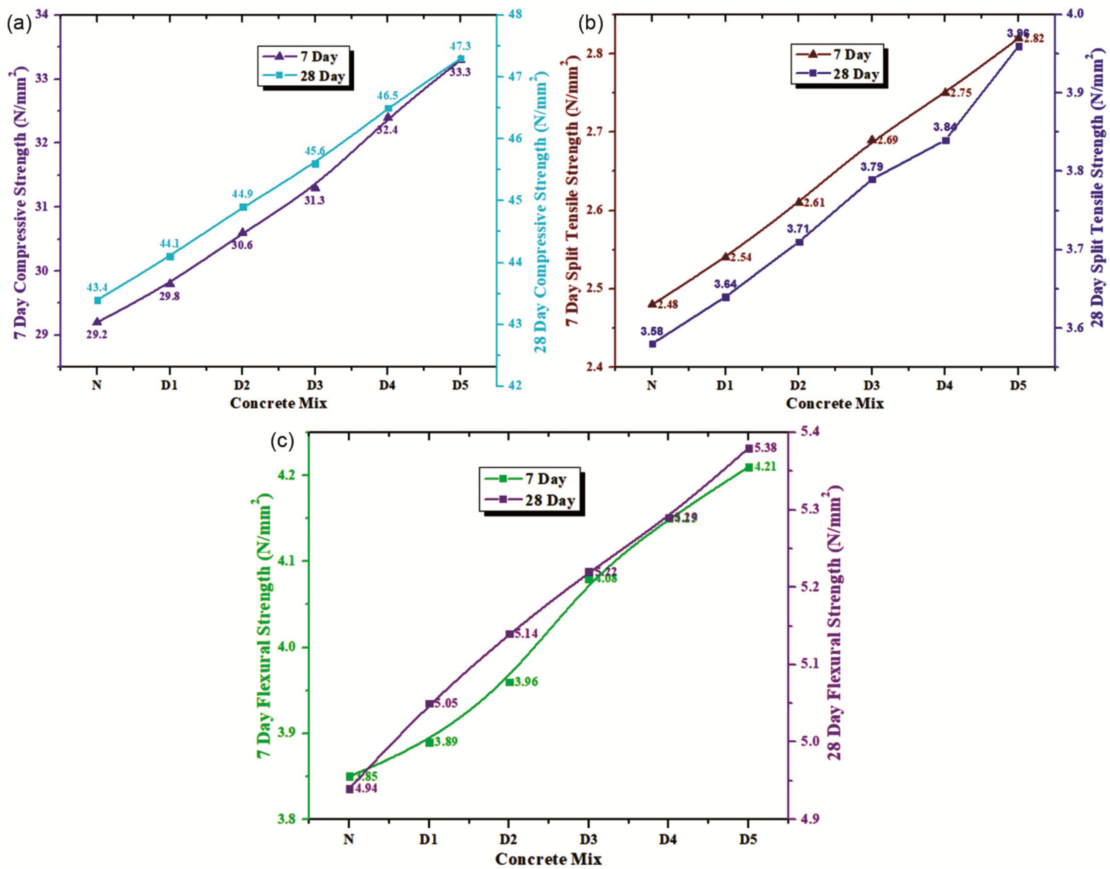


Fig. 9 — Effect on strength parameters of FA+MSF+WRA (12M) replacement (a) Compressive strength, (b) Split tensile strength and (c) Flexural strength.

higher[33-35]. Further, the strength parameter also depends on the molarity of alkaline activator solutions. It was found that using 8M of alkaline activator led to an optimal mix with 92-8% FA+MSF whereas 12M alkaline activator solution gave 8-12% FA+MSF as optimal mix with desirable strength parameters similar to the previous studies[36-38]. From the analysis of the results, it was decided that the most optimum mixes were A2, B3, C2, and D3, which are all blends consisting of varying proportions of additional components. These blends have been chosen for future exploration.

### 3.4 Microstructure analysis of optimum mixes

SEM analysis of four optimally selected mixes namely A2, B3, C2, and D3 was carried out to determine their microstructural properties as shown in Fig. 10. It is clear from these images that the paste containing 12% MSF (D3 mix) has a more dense microstructure and a matrix that is almost completely reacted, whereas, few MSF particles have not reacted in the cenosphere and plerosphere sections[6, 39]. The unreacted particles do not perform the function of filler in the mixture; rather, they contribute to an increase in the matrix's strength[40-42].

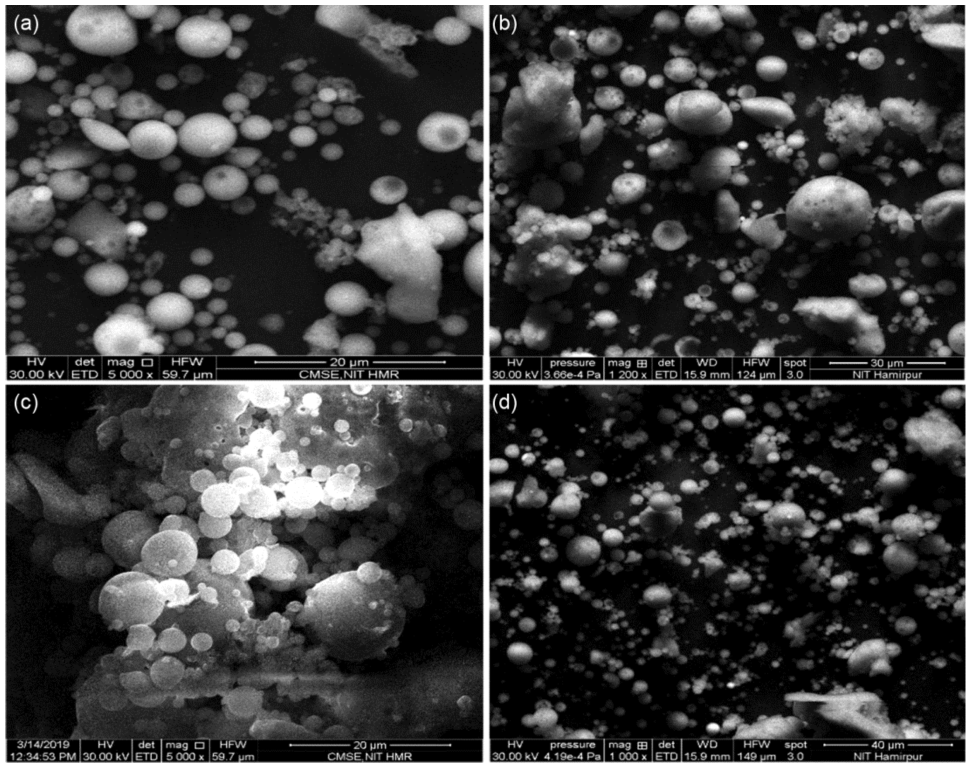


Fig. 10 — Microstructure analysis of (a) A2, (b) B3, (c) C2 and (d) D3.

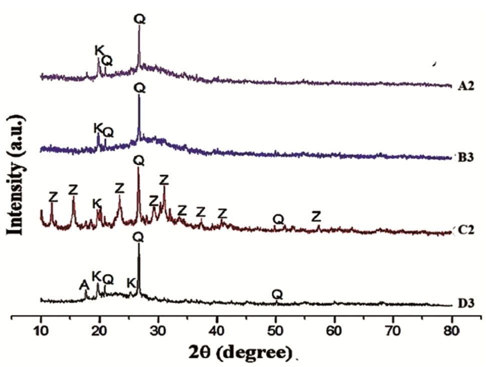


Fig. 11 — XRD analysis of optimum concrete mixes (a) A2, (b) B3, (c) C2, and, (d) D3.

The XRD analysis of the optimal design mixes, depicted in Fig. 11, revealed the existence of quartz (Q), nepheline (A), bavenite (K) and CSH phases. Quartz is a silica-based oxide, while nepheline is a sodium alumino-sulphate hydrate that possesses strength, a key determinant of the geopolymer mechanism. Bavenite (K), in this context, denotes calcium-based hydration compounds known as CASH, which are formed from the interaction of calcium with the alkalis present in the geopolymer mixture. The presence of both non-alcoholic steatohepatitis (NASH) and chronic sinusoidal hepatic (CSH) and chronic alcoholic steatohepatitis (CASH) affects the strength and permeability characteristics of the glomerular capillary wall (GPC)[43-44].

In addition, the activity of MFS is greater when compared to the activity of FA, and the reaction that is caused by the alkali is an exothermic process. The heat produced, speeds up the geopolymerisation process, which allows the production of a greater quantity of gel products in a shorter amount of time. By doing so, the holes that exist between the particles can be filled, resulting in a denser microstructure. When the number of WRA in the mixture is increased to 40%, it has been observed that the gel-like hydration products intensely increased, and the mechanical characteristics significantly improves. It was also determined that an excessive amount of WRA increased the drying shrinkage of the material, which in turn led to a deterioration in its durability[45-47]. Hence, D3 mix has found to have better microstructural properties with optimal mechanical characteristics among all the geopolymer mixes.

## 4 Conclusion

In the present study, FA based GPC has been made using low in calcium dry fly ash (ASTM Class F). The sodium silicate solution and the sodium hydroxide particles in pellet form were mixed to generate the alkaline liquid. WRA were utilized as coarse aggregate replacements. This study's combination proportions were refined from earlier research on GPC using FA[48-50]. For comparison, alkaline binder solutions with molarities of 8M and 12M were used. A mass ratio of $Na_2SiO_3$/NaOH at 2.5 was set to establish the activator solution that react with FA. The following conclusions are made based on the experimental work described in this study:

a For achieving high strength and durability, the nominal mix was approved with several modifications. To have an efficient casting process and an increase in strength, it is necessary to have the optimal mix proportions that have an adequate setting time, sorptivity and water absorption.

b Experimental examination using the slump cone test clearly showed that the constituents of GPC greatly affect the workability. Because of its pozzolanic character, FA and MSF decreases workability as compared to regular Portland cement. Nevertheless, the optimal mix percentage, along with all the other mix proportions, had a reasonable slump value, indicating acceptable workability.

c A comprehensive experimental analysis was performed on the compressive, flexural, and splitting tensile strengths of modified GPC for every trial mix percentage. When FA and MSF were combined with 12M alkaline binder, there was a noticeable rise in the strength of the material. As a consequence, obtaining 92-8% FA+MSF 12M (B3), it achieves a maximum compressive strength of 45.2 N/mm$^2$, a flexural strength of 5.14 N/mm$^2$, and a splitting tensile strength of 3.88 N/mm$^2$ in a period of 28 days.

d The study also revealed that choosing an adequate molarity of alkaline binder solution is very important. Out of 8M and 12M blend of sodium silicate ($Na_2SiO_3$) and sodium hydroxide (NaOH) with mass ratio of 2.5, the 12M binder solution performed better than 8M in terms of overall fresh and mechanical properties of the GPC mixes.

e The presence of MSF in the polymerization reaction and its subsequent dissolution to produce amorphous solids is demonstrated in samples of modified GPC that substitute FA with MSF. Because of its pozzolanic properties, MSF has been important in avoiding shrinkage fractures, as shown in the SEM micrograph.

f The microstructural analysis also revealed a positive impact of supplementary material inclusion in GPC. The gel-like hydration characteristics were frequently observed which resulted in better geopolymerisation and adequate adhesion among the constituent materials especially in the optimal D3 (FA 88%; MSF 12%; WRA 30%; 12M) mixture.

g The cost analysis of the geopolymer mixes indicated a reduction in cost of production of 1 m$^3$ of GPC in all the mixes. However, incorporating FA, MSF and WRA combinedly reduced the cost substantially for 17.32% in C2 and 14.84% in D3 mix of GPC.

## References


1 Duan P, Yan C, Zhou W & Ren D, *Ceram Int*, 42 (2016) 13507.

2 Saptamongkol A, Sata V, Wongsa A, Kroehong W, Ekprasert J & Chindaprasirt P, *J Build Eng*, 76 (2023) 107245.

3 Davidovits & Joseph, *J Therm Anal*, 37 (1991) 1633.

4 Jawad A, Kontoleon K J, Majdi A, Naqash M T, Deifalla A F, Kahla N B, Isleem H F & Qaidi S M A, *Sustainability*, 14 (2022) 8783.

5 Amran M, Fediuk R, Murali G, Avudaiappan S, Ozbakkaloglu T, Vatin N, Karelina M, Klyuev S, & Gholampour A, *Materials*, 14 (2021) 4264.

6 Ismail I, Bernal S A, Provis J L, Hamdan S & Deventer J S J V, *Mater Struct*, 46 (2013) 361.

7 Ahmadi B & Shekarchi M, *Cem Concr Compos*, 32 (2010) 134.

8 Panda B, Singh G V P B, Unluer C & Tan M J, *J Clean Prod*, 220 (2019) 610.

9 Pires E F C, Lima T V, Marinho F J V, Vargas A S D, Mounzer E C, Darwish F A I & Silva F J, *Integr Med Res*, 8 (2019) 2083.

10 Rosenfeld A H, Akbari H, Bretz S, Fishman B L, Kurn D M, Sailor D & Taha H, *ENB*, 22 (1995) 255.

11 Mendes B, Andrade I K R, Carvalho J M F D, Pedroti L & Júnior A D O, *Int J Appl Ceram Technol*, 18 (2021) 262.

12 Amran Y H M, Alyousef R, Alabduljabbar H & El-Zeadani M, *J Clean Prod*, 251 (2020) 119679.

13 Li B, Gao A, Li Y, Xiao H, Chen N, Xia D, Wang S & Li C, *Constr Build Mater*, 60 (2022) 11.

14 Okoye F N, Durgaprasad J & Singh N B, *Ceram Int*, 42 (2016) 3000.

15 Karakoç M B, Türkmen I, Maraş M M, Kantarci F, Demirboğa R & Toprak M U, *Constr Build Mater*, 72 (2014) 283.

16 Bignozzi M C, Manzi S, Natali M E, Rickard W D A & Riessen A V, *Constr Build Mater*, 69 (2014) 262.

17 Duxson P, Lukey G C & Deventer J S J V, *J Mater Sci*, 42 (2007) 3044.

18 Tchakoute H K, Elimbi A, Kenne B B D, Mbey J A & Njopwouo D, *Ceram Int*, 39 (2013) 269.

19 Yao X, Zhang Z, Zhu H & Chen Y, *Thermochim Acta*, 493 (2009) 49.

20 Xie Z & Xi Y, *Cem Concr Res*, 31 (2001) 1245.
21 Hong F, Yu S, Hou D, Li Z, Sun H, Wang P & Wang M, *J Build Eng*, 79 (2023) 107705.
22 Chindaprasirt P, Chareerat T & Sirivivatnanon V, *Cem Concr Compos*, 29 (2007) 224.
23 Nath P & Sarker P K, *Constr Build Mater*, 66 (2014) 163.
24 Qureshi M N & Ghosh S, *Adv Civil Eng Mater*, 2 (2013) 62.
25 Karakoç M B, Türkmen I, Maraş M M, Kantarci F & Demirboğa R, *Ceram Int*, 42 (2016) 1254.
26 Deb P S, Sarker P K & Barbhuiya S, *Cem Concr Compos*, 72 (2016) 235.
27 Sharmila P & Dhinakaran G, *Constr Build Mater*, 129 (2016) 48.
28 Kaniraj S R & Havanagi V G, *Cem Concr Res*, 29 (1999) 673.
29 Azevedo F, Pacheco-Torgal F, Jesus C, Barroso De Aguiar J L B D & Camões A F, *Constr Build Mater*, 34 (2012) 186.
30 Li L J, Tu G R, Lan C & Liu F, *J Clean Prod*, 124 (2016) 325.
31 Almutairi A L, Tayeh B A, Adesina A, Isleem H F & Zeyad A M, *Case Stud Constr Mater*, 15 (2021) e00733.
32 Zhang D, Wang X, Kang S, Cheng G and Wu W, *Case Stud Constr Mater*, 19 (2023) e02284.
33 Ducman V & Korat L, *Mater Charact*, 113 (2016) 207.
34 Guo X & Pan X, *Constr Build Mater*, 179 (2018) 633.
35 Sumajouw D M J, Hardjito D, Wallah S E & Rangan B V, *J Mater Sci*, 42 (2007) 3124.
36 Zhang J, Fu Y, Wang A & Dong B, *Constr Build Mater*, 385 (2023) 131530.
37 Assi L N, Deaver E, Elbatanouny M K & Ziehl P, *Constr Build Mater*, 112 (2016) 807.
38 Shi X S, Collins F G, Zhao X L & Wang Q Y, *J Hazard Mater*, 237 (2012) 20.
39 Puertas F & Jiménez A F, *Cem Concr Compos*, 25 (2003) 287.
40 Arioz E, Arioz O & Kockar O M, *Procedia Eng*, 42 (2012)100.
41 Guo X, Shi H & Dick W A, *Cem Concr Compos*, 32 (2010) 142.
42 Yunsheng Z, Wei S & Zongjin L, *Appl Clay Sci*, 47 (2010) 271.
43 Al-mashhadani M M, Canpolat O, Aygörmez Y, Uysal M & Erdem S, *Constr Build Mater*, 167 (2018) 505.
44 Aydin S & Baradan B, *Mater Des*, 35 (2012) 374.
45 Kumar P, Pankar C, Manish D & Santhi A S, *Mater Today: Proc*, 5 (2018) 28127.
46 Salih M A, Abdullah A, Ali A & Farzadnia N, *Constr Build Mater*, 65 (2014) 592.
47 Zhang Z, Provis J L, Ma X, Reid A & Wang H, *Cem Concr Compos*, 92 (2018) 165.
48 Zejak R, Nikolić I, Blečić D, Radmilović V and Radmilović V, *Mater tehnol*, 47 (2013) 535.
49 Narayanan A & Shanmugasundaram P, *ENB*, 138 (2017) 539.
50 Labaied I, Douzane O, Lajili M & Promis G, *RILEM Bookseries*, 45 (2023) 54.